International Journal of Refrigeration 89 (2018) 40–50

Contents lists available at ScienceDirect

International Journal of Refrigeration

journal homepage: www.elsevier.com/locate/ijrefrig

Experimental study on the effect of Zirconia nanoparticles on solidification heat transfer characteristics: A comparison with Titania nanoparticles

Hoda Aslani, Mohammad Moghiman*

Department of Mechanical Engineering, Ferdowsi University of Mashhad, Mashhad, Iran

ARTICLE INFO

Article history:
Received 25 August 2017
Revised 11 December 2017
Accepted 14 January 2018
Available online 31 January 2018

Keywords:
Solidification
Nucleation
Supercooling degree
Nanofluid
Surfactant
Phase change material

ABSTRACT

In this study, the influence of Zirconia (ZrO_2) and Titania (TiO_2) nanopaticles on liquid–solid phase transition of aqueous nanofluids with/without Poly vinyl pyrrolidone as surfactant are experimentally compared. A cooling generation apparatus based on the compression refrigeration cycle has been used to explore the solidification behavior of nanofluids as phase change materials. The experimental results show that ZrO_2 and TiO_2 nanoparticles considerably reduce the solidification supercooling degree of deionized water (as basefluid). Only adding 0.04 wt% ZrO_2 and TiO_2 nanoparticles to base fluid, the percentage of reduction in supercooling degree attained 81% and 65%, respectively. The results reveal that although the presence of surfactant in nanofluids reduces the supercooling degree and slightly solidification time of both ZrO_2 and TiO_2 nanofluids; but it has no influence on onset nucleation time. Comparison of ZrO_2 and TiO_2 nanofluids with/without surfactant presents that ZrO_2 provides faster solid layers formation and has more energy saving potential in storage systems due to its lower supercooling degree.

Étude expérimentale de l'effet de nanoparticules de zirconium sur les caractéristiques de transfert de chaleur par solidification: comparaison avec les nanoparticules de titane

Mots-clés: Solidification; Nucléation; Degré de surfusion; Nanofluide; Tensioactif; Matériau à changement de phase

1. Introduction

Application of Phase Change Material (PCM) to store and release latent heat in energy storage systems as an efficient method, allows high energy storage capacity and massive charge/discharge rate (Nomura et al., 2016; Lei et al., 2016; Elmozughi et al., 2014; Abdollahzadeh and Esmaeilpour, 2015). Various techniques have been proposed and investigated to improve operation of energy storage system by enhancing thermal conductivity of PCMs such as introducing metal structures into PCM, dispersing micro particles into PCM and using double layer network for Phase change composites (Wang et al., 2016a; Wang et al., 2016b; Golestaneh et al., 2016).

Nowadays, due to rapid development of nanotechnology, the thermophysical properties of PCMs in the presence of nanoparticles (Yiamsawasd et al., 2012; Raja et al., 2016; Mahbubul et al., 2013) and likewise phase changing process of nanofluids (Kim et al., 2011; Moghiman and Aslani, 2013; Altohamy et al., 2015) have attracted significant research attention. Preliminary evidences indicated that the aqueous nanofluid could be an effective material to modify the performance of cooling energy storage system (Chandrasekaran et al., 2014b; Mo et al., 2012); because nanoparticles act as nucleating agent to promote solidification rate by improving heterogeneous nucleation (which takes place in

Abbreviations: COP, coefficient of performance; DNSD, dimensionless number of supercoiling degree; DNST, dimensionless number of solidification time; DW, deionized water; ONT, onset nucleation time, S; PCM, phase change material; PVP, poly vinyl pyrrolidone; SD, supercoiling degree, °C; ST, solidification time, S.

* Corresponding author.
E-mail addresses: aslani_hoda@yahoo.co.in (H. Aslani), moghiman@um.ac.ir (M. Moghiman).

https://doi.org/10.1016/j.ijrefrig.2018.01.009
0140-7007/

Nomenclature

ΔG	Gibbs potential variation, kJ
Δg_v	volumetric free energy, kJ m^{-3}
Δh	mass specific phase change enthalpy, kJ kg^{-1} K^{-1}
K	thermal conductivity, W m^{-1} K^{-1}
r	radius, m
r^*	critical nucleation radius, nm
T	temperature, K
T_m	phase change temperature, K
T_n	nucleation temperature, K
W	power, W

Greek symbols

γ	interface free energy, kJ m^{-2}
γ_{iw}	ice-water interface free energy, kJ m^{-2}
η	efficiency
θ	contact angle, °
μ	dynamic viscosity, kg m^{-1} s^{-1}
υ	kinematic viscosity, m^2 s^{-1}
ρ	density, kg m^{-3}
ϕ	volume fraction

Subscripts

A	ambient
BF	basefluid
Cons	consumption
E	evaporator
N	net
NF	nanofluid
NP	nanoparticle
P	particle

nanofluids). The recent investigations revealed that the presence of Alumina, Copper oxide, TiO_2, graphene oxide nanoparticles and multi-walled carbon nanotubes in basefluid would reduce the Supercooling Degree (*SD)* with an advance in the onset nucleation time (*ONT*) and a decrease in the solidification time (*ST*) (Altohamy et al., 2015; Chandrasekaran et al., 2014a; Chandrasekaran et al., 2014b; Mo et al., 2012; Aslani and Moghiman, 2015; Teng, 2013; Wu et al., 2009; Mo et al., 2015; Harikrishnan et al., 2013; Jia et al., 2014; Fan et al., 2015; Kumaresan et al., 2013; Kumaresan et al., 2012), but the lack of direct comparison makes conclusions hard to interpret.

In addition to nanoparticles, surfactants can be used to reduce the *SD* of nanofluids (Wu et al., 2009; Jia et al., 2014). According to the theoretical analysis of heterogeneous nucleation associated with surfactants, Wu et al. (2009) and Jia et al. (2014) showed that the addition of sodium dodecyl benzene sulfonate and sodium dodecylsulfate as surfactants could reduce the *SD* of nanofluids due to the reduction in free energy change required for nucleation. Furthermore, Wang et al. (2014) and Zhang et al. (2010) considered the relation between free energy change and nucleation behavior in Copper, Alumina and Silica nanofluids. As will be discussed in detail in Section 2, solidification proceeding and *SD* are relevant to critical nucleation radius (r^*), therefore, Liu et al. (2015) investigated the critical nucleation radius in graphene oxide nanofluid under nucleation process. They tabulated the critical nucleation radius of graphene oxide nanofluid based on the nanoparticle concentrations.

Further to play nucleating agent role by nanoparticles to reducing *SD*, inadequate efforts have been put in for exhibiting the effects of nanoparticle structure and properties on solidification heat transfer characteristics (Abdollahzadeh and Esmaeilpour, 2015; Liu et al., 2015; Zhao et al., 2013). Nanoparticles, influence on heat transfer characteristics of basefluid enhancing kinematic viscosity, changing thermal conductivity and suppressing the turbulence (Kumaresan et al., 2012; Khodadadi et al., 2013). According to the literatures, the measurement of viscosity of nanofluids is performed by cone and plate viscometer. Also, thermal conductivity is measured by transient hot wire method. The measurement of latent heat (and specific heat) is performed by differential scanning calorimetry (He et al., 2012). Based on these measurements, the required empirical equations are presented in Section 2. The lower enhancement in viscosity of nanofluid accompanied by a higher heat transfer, leads to lower time requirement for complete solidification (Harikrishnan et al., 2013; Kumaresan et al., 2012).

Numerous confirmatory studies of the effects of various parameters on solidification behavior of TiO_2 nanofluids (Mo et al., 2012; Mo et al., 2015; Harikrishnan et al., 2013; Jia et al., 2014; Aslani and Moghiman, 2015), makes it useful to compare as an additive to basefluid. In order to extend the existing knowledge in the field of nanofluid solidification process, the present research work aims to explore and compare the solidification heat transfer characteristics of ZrO_2 as low kinematic viscosity nanofluid with TiO_2 nanofluid with/without Poly Vinyl Pyrrolidone (PVP) as a surfactant. Despite of cubic molecular structure and symmetric bonds of ZrO_2, which make it suitable for heat transfer applications (Sarafraz et al., 2016), the literature reviewed demonstrates that the solidification behavior of Deionized Water (DW) dispersed with the ZrO_2 nanoparticles has not been reported. In sum, ZrO_2 is selected to investigate, due to its low kinematic viscosity and its structure (suitable for heat transfer applications). The selection of TiO_2 nanoparticles is due to numerous confirmatory studies on it (suitable to comparison).

2. Mechanisms and evaluation of phase change

To analyze solidification characteristics, three stages of process should be deliberated as (Li et al., 2013; Wang et al., 2014; Yamanaka et al., 2012): (1) nucleation occurrence by reducing the fluid temperature to the nucleation temperature (T_n) and (2) growth of nucleation and crystal formation by enhancing the fluid temperature to the phase change temperature (T_m). (3) formation of solid layers by releasing latent heat at a constant temperature of T_m (Phase transition) in solidification time. The appearance of crystal nuclei is closely related to the Gibbs free energy variation (Wang et al., 2014). The Gibbs potential variation (ΔG) due to the new phase formation for a spherical droplet of radius (r) is as follows (Gunther et al., 2011):

$$\Delta G\ (r,\ T) = \frac{4}{3}\pi r^3 \rho\, \Delta h \left(\frac{T}{T_m} - 1\right) + 4\pi r^2 \gamma \tag{1}$$

where ρ denotes the density, Δh and T_m are the mass specific phase change enthalpy and phase change temperature and γ stands for the interface free energy which depends upon solid–liquid interface created in the course of phase transition.

As surfactants contribute to change the structure of the droplet surface, Eq. (1) that can be applied for the case of nucleation on a spherical droplet, must be reconstructed to determine the Δg_v:

$$\Delta G\ (r,\ T, \theta) = \frac{4}{3}\pi r^3 \rho\, \Delta h \left(\frac{T}{T_m} - 1\right) F(\theta) + 4\pi r^2 \gamma f(\theta) \tag{2}$$

where θ refers to contact angle and both $F(\theta)$ and $f(\theta)$ are functions of contact angle (Zhang et al., 2010).

The first term on the right-hand side of Eqs. (1) and (2) refers to volumetric term whereas the second one refers to surface term. Volumetric free energy (Δg_v) reversely influence on r^*. Radius of formed new phase (solid nucleate) in main phase (liquid) grows spontaneously beyond a certain cluster size, r^*, introduced as (Liu

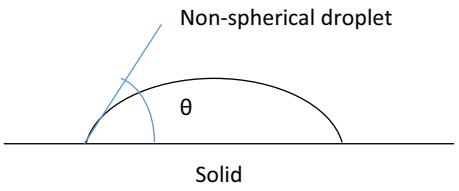

Fig. 1. The physical model of contact angle in droplet nucleation.

et al., 2015):

$$r^* = -\frac{2\gamma_{iw}}{\Delta g_v} \tag{3}$$

in which, γ_{iw} corresponds to the ice–water interface free energy and in term of γ_{iw}, the value of $2.3^{*}10^{-5}$ kJ m^{-2} referred to the literature conducted by Liu et al. (2015). Also, Δg_v of basefluid and nanofluid can be expressed as:

$$\Delta g_v = \frac{-\rho \times \Delta h \times SD}{T_m} \tag{4}$$

where ρ and Δh of nanofluids are calculated from following empirical formulas (Bavand et al., 2015; Zabalegui et al., 2014). Empirical equation for Δh (used in this work) is derived from results tested by differential scanning calorimetry; but due to low concentrations of nanoparticles, the effect of additives on mass specific phase change enthalpy is negligible and it can be considered as a constant value for DW and nanofluids, according to the literature of Liu et al. (2015).

$$\rho_{NF} = (1 - \emptyset_P) \times \rho_{BF} + \emptyset_P \times \rho_{NP} \tag{5}$$

$$\Delta h_{NF} = \frac{\rho_{BF} \times \Delta h_{BF}(1 - \emptyset_P)}{\rho_{NF}} \tag{6}$$

where ϕ_P refers to the volume fraction of additives and obtained from Eq. (7) and For DW as basefluid, ρ = 999 kg m^{-3} and Δh = 334.38 kJ kg^{-1} (Liu et al., 2015; Khodadadi et al., 2013).

$$\emptyset_P = \frac{\rho_{BF} \times \text{wt\%}}{\rho_{BF} \times \text{wt\%} + (1 - \text{wt\%}) \times \rho_P} \tag{7}$$

According to Eq. (8), *SD* represents the difference between the phase change temperature and nucleation temperature (Liu et al., 2015). It is important to note that the considerable effect of additives on Δg_v is emerged in *SD*.

$$SD = T_m - T_n \tag{8}$$

where T_n is nucleation temperature.

As briefly mentioned in Section 1, it is important to find and determine the dominant mechanism in various experiments. It is evident in reviewing the literature that there are four major mechanisms which play roles in controlling solidification behavior (Zhang et al., 2010; Zabalegui et al., 2014; Mo et al., 2015; Wang et al., 2016a).

1) Effect of nucleating agent: additives including nanoparticles and/or surfactants into PCMs can provide nucleating sites of liquid by solid–liquid interface and solid particles surface which suspended in PCM (Mo et al., 2015). In other words, additives operate as agent of nucleation to induce surface nucleation, especially at higher concentrations of additives.
2) Effect of contact angle: reduction of contact angle from $\theta = 180°$ in spherical droplets, leads to enhancement of contact surface area and reduction of Gibbs free energy variation. As solid–liquid interfaces are nucleating sites of liquid, contact surface area enhancement facilitates nucleation proceeding. Therefore non-spherical droplets (see Fig. 1) need less cooling energy compared to spherical droplets and nucleation occurs in higher temperature (T_n) and consequently lower *SD* (Eq. (8)) (Zhang et al., 2010). Hence, *SD* implicitly depends on contact angle. Also, as Gibbs free energy is constant ($\Delta G = 0$) during phase change process, change in contact angle and consequently reduction of ΔG (due to surfactant additives), accelerates the phase change process and enhance the rate of released latent heat and implicitly reduce *ST* (Wu et al., 2009; Jia et al., 2014).
3) Effect of thermal conductivity: additives with higher thermal conductivity such as metal/metal oxide nanoparticles provide a higher rate of conduction heat transfer and accelerate solidification process (Wang et al., 2016a).
4) Effect of kinematic viscosity: in general, nanoparticle additives enhance kinematic viscosity which is a contrary mechanism in heat transfer. It occurs because a decrease in kinematic viscosity intensify Brownian motion which significantly elevates buoyancy-driven convection (on account of Grashof number), facilitates latent heat reduction (Zabalegui et al., 2014). If the relative weight of natural convection to heat conduction in solidification process can promote solidification behavior, the concentration of nanoparticle is well within the safe range connected with viscosity (Zeng et al., 2013).

Therefore, it is important to take into account contrast mechanism to choose nanoparticles (Kumaresan et al., 2012). Optimal choice is found when nanoparticles have higher thermal conductivity and lower kinematic viscosity in optimum concentrations to adjust mechanisms in desire conditions. An enhancement of nanoparticle concentration, leads to change in thermal conductivity of PCM, increase in nucleating sites and kinematic viscosity; but lower enhancement of kinematic viscosity is desired. Therefore, various experimental works should be conducted to determine the dominant mechanism in solidification behavior of nanofluids.

In order to facilitate fair and comprehensive comparison between important parameters of solidification in nanofluids, dimensionless numbers of *SD* (*DNSD*) and *ST* (*DNST*) are defined as a ratio of *SD* and *ST* of nanofluids to that of their basefluid (DW) and are represented as follows:

$$DNSD = \frac{SD_{NF}}{SD_{BF}} \tag{9}$$

$$DNST = \frac{ST_{NF}}{ST_{BF}} \tag{10}$$

Investigations of solidification behavior require consideration of efficiency and performance of cooling energy storage systems. Higher efficiency (η) of energy storage system is obtained in lower *SD*; and also depends on energy storage rate, thermal stability and thermal conductivity of PCMs (Lu and Tassou, 2012; Sari et al., 2014; Wang et al., 2016b). The efficiency of the energy storage system is the cold exergy efficiency i.e. net power generation (W_N) to electricity power consumption (W_{Cons}). The efficiency and coefficient of performance (*COP*) in the energy storage system are expressed as:

$$\eta = \frac{W_N}{W_{cons}} \tag{11}$$

$$COP = \eta \frac{1}{\frac{T_A}{T_E} - 1} \tag{12}$$

where T_A and T_E denote ambient temperature and evaporator temperature, respectively (Du and Ding, 2017).

From Eqs. (11) and (8), it is clearly deduced that higher T_n and consequently lower *SD* will result in higher temperature of evaporator operation and therefore lower electricity consumption which make saving on energy. Also, it is elucidated from Eq. (12), that *COP* enhancement of energy storage system is caused by higher T_E

Table 1
Thermophysical properties of TiO_2 and ZrO_2 nanoparticles (Azmi et al., 2016; Williams et al., 2008; Ismail et al., 2012).

NP	Size nm	wt%	K_{nf} (W m^{-1} K^{-1})	K_{nf}/K_{bf}	$\rho_{nf} * 10^{-3}$ (kg m^{-3})	ρ_{nf}/ρ_{bf}	$\mu_{nf} * 10^{3}$ (kg m^{-1} s^{-1})	μ_{nf}/μ_{bf}	$\upsilon_{nf} * 10^{7}$ (m^2 s^{-1})	$\upsilon_{nf}/\upsilon_{bf}$
ZrO_2	20	0.04	0.600	1.016	5.895	5.901	2.423	1.356	4.110	0.230
TiO_2	20	0.04	0.608	1.030	3.903	3.907	1.912	1.070	4.899	0.274

(higher T_n and lower *SD*) and higher efficiency, too. On the other hand, the reduction of *ST* and/or *ONT* will enhance the *COP* by enhancing W_N and η.

3. Experimental measurements

3.1. Nanofluid preparation

In this study, two-step method for preparing nanofluids was used. Producing nanoparticles as dry powders and then at the second processing step, dispersing nano-sized powders into the base fluid were performed in this method. Sonication in nanofluid preparation was used to reduce particle agglomeration and enhance stability of the suspension (Moghiman and Aslani, 2013). In this experimental investigation, TiO_2 and ZrO_2 nanoparticles (0.01, 0.02 and 0.04 wt%) were used (thermophysical properties are given in Table 1). In practical scenario, the only nanoparticle weight required for 100 kg DW is 40 g (for 0.04 wt%) and their costs are about 70 and 150 $ for TiO_2 and ZrO_2, respectively, which enhancement of *COP* and η by reducing electricity power consumption is able to compensate the nanoparticles costs.

Nanoparticles were mixed with DW as base fluid by magnetic stirrer for 15 min at the speed of 450 rpm and sonicated by an ultrasonic homogenizer (50 kHz) for 30 min. These spherical nanoparticles were weighed by an electronic balance whose precision is ±0.001 g.

It is clearly evident that extremely low concentration of nanofluids is more stable than higher concentrations. Even though nanofluid preparation without ultrasonic homogenizer gradually causes aggregation and sedimentation of nanoparticles, the presence of nanoparticles (even in sediment form) leads to heat transfer enhancement, due to their high surface-to-volume ratio.

3.2. Experimental apparatus and procedure

Fig. 2 illustrates the experimental setup to investigate solidification process of nanofluids. This setup consists of a cooling system based on compression refrigeration cycle, thermally insulated tank, *K*-type thermocouple and data logger. Insulated tank of 10 L capacity was filled with a mixture of 25% ethylene glycol and 75% water by volume (freezing phase change temperature of −12 °C). A *K*-type thermocouple with an accuracy of ±0.01 °C was implemented to control the mixture temperature to be at −12 °C. A cylindrical polyethylene test section (80 mm in diameter and 200CC in volume) placed at insulated tank, was used to study nanofluid solidification behavior. To continuously monitor the temperature variation of the nanofluid (every 1 min.), *K*-type thermocouple with an accuracy of ±0.01 °C was located at the center of test section. Prior to performing the experiments, measuring instruments had been calibrated and the experiments were repeated three times. The uncertainty of nanofluid temperature and mass was estimated to be 4% and 0.1%, respectively.

4. Results and discussion

4.1. Solidification process of ZrO_2 and TiO_2 nanofluids

The temperature variation of ZrO_2 nanofluid versus time at different nanoparticle concentrations (DW = 0, 0.01, 0.02 and 0.04 wt%) is plotted in Fig. 3. It is observed that the ZrO_2 nanoparticle helps to advance in onset nucleation time (*ONT*) and reduce the solidification time (*ST*) and supercooling degree (*SD*) which improve efficiency and performance of cooling energy storage (according to the definition of η and *COP* based on Eqs. (11) and (12)). This occurs because the nanoparticles act as nucleating agent and consequently accelerate the nucleation process. This result is consistent with the previous report carried out on TiO_2 (Aslani and Moghiman, 2015) which to facilitate comparison, presented in Fig. 4. According to Table 1, ZrO_2 and TiO_2 as metal oxide nanoparticles enhance thermal conductivity of nanofluids and as a result, elevate the rate of releasing latent heat and the solid layers formation. The maximum enhancement in *ONT* and reduction in *ST* is found to be in maximum used nanoparticle concentration (0.04 wt%). The comparison between Figs. 3 and 4 indicates that ZrO_2 nanofluid contributes to lower *SD* and *ONT*. Now, it is noteworthy to compare and discuss solidification behavior of ZrO_2 and TiO_2 nanofluids, in detail.

4.2. Comparison of solidification characteristics of ZrO_2 and TiO_2 nanofluids

Comparison of *SD* between ZrO_2 and TiO_2 nanofluids is presented in Fig. 5. It can be seen that an increase in concentrations of both nanoparticles, reduces the *SD* of nanofluids. The results show that for 0.04 wt% concentration of two nanoparticles, *SD* is reduced by 81% in the case of ZrO_2 nanofluid whereas the reduction of *SD* in TiO_2 is only about 65%. It is due to the fact that nanoparticles in basefluid have tendency to increase nucleating surface sites by enhancing nucleating agent and reducing contact angle. Also, metal oxide nanoparticles enhance thermal conductivity of nanofluids. In turn, through four major mechanisms of controlling solidification behavior, contemporary growth of these three mechanisms improve solidification characteristics of DW (especially *SD*); meanwhile, because of deteriorate effect of kinematic viscosity enhancement in the presence of nanoparticles (Azmi et al., 2016), lower enhancement of ZrO_2 kinematic viscosity (see Table 1) and consequently lower thermal dispersion (because of Brownian motion) leads to lower *SD* and higher saving energy in solidification process of ZrO_2 compared to Tio_2. It should be considered that as quantities of thermal conductivity and kinematic viscosity have different order of magnitude, relative difference or ratio of values are used to compare. From Table 1, it is evident that difference of kinematic viscosity ratio between nanofluids is higher than that of thermal conductivity. Owing to this attributes, kinematic viscosity has been found to be a dominant mechanism in introducing ZrO_2 as emerging candidate of PCM in energy storage systems, (in contrast with the effect of relatively higher thermal conductivity of TiO_2).

Fig. 6 illustrates the comparison of *DNSD* between ZrO_2 and TiO_2 nanofluids with respect to *DNST*. According to the slope of ZrO_2 and TiO_2 curves in Fig. 6, it is inferred that the effect of nanoparticle additives on the reduction of *DNSD* is greater than that of *DNST* especially in ZrO_2. A reduction of nearly 80% and 60% in the *DNSD* of ZrO_2 and TiO_2 along with a reduced *DNST* of 20% is observed in Fig. 6. The prevailing effect of ZrO_2 on nucleation step (relevant to *SD*) compared with solid layer formation (relevant to *ST*) is deduced from the results of Fig. 6.

Fig. 7 presents both the *ONT* and *ST* of ZrO_2 and TiO_2 nanofluids at various nanoparticle concentrations. The results show that extremely low concentration of ZrO_2 and TiO_2 nanoparti-

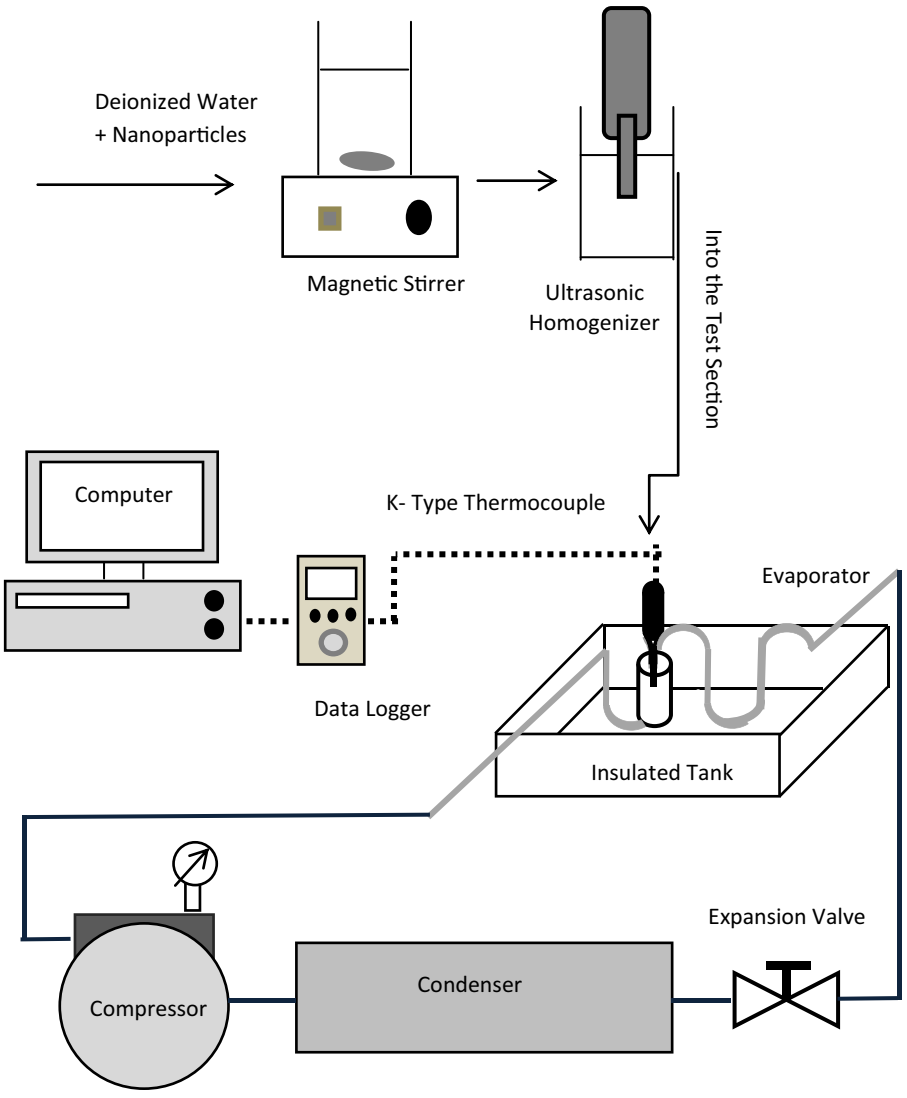

Fig. 2. Schematic diagram of the experimental setup.

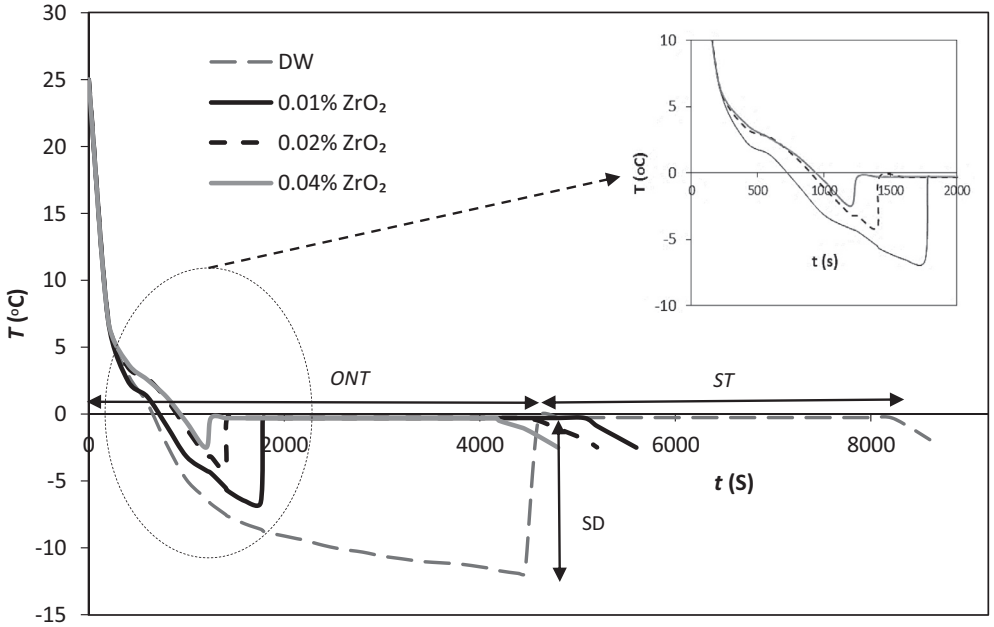

Fig. 3. Effect of ZrO_2 nanoparticle concentrations on timewise variation of nanofluid cooling curve.

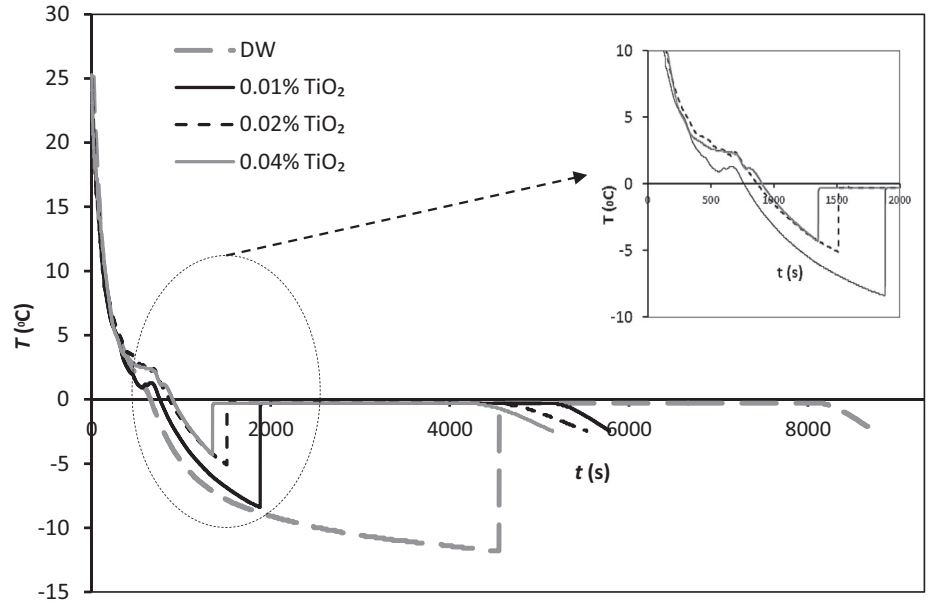

Fig. 4. Effect of TiO_2 nanoparticle concentrations on timewise variation of nanofluid cooling curve (Aslani and Moghiman, 2015).

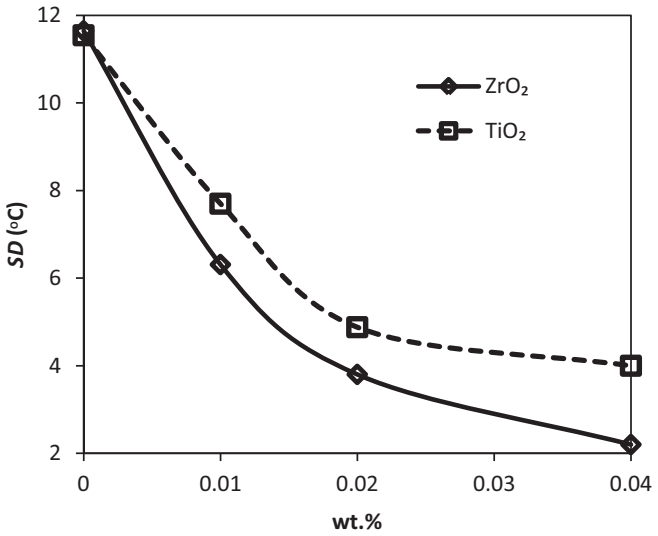

Fig. 5. Comparison of *SD* between ZrO_2 and TiO_2 nanofluids with respect to nanoparticle concentration.

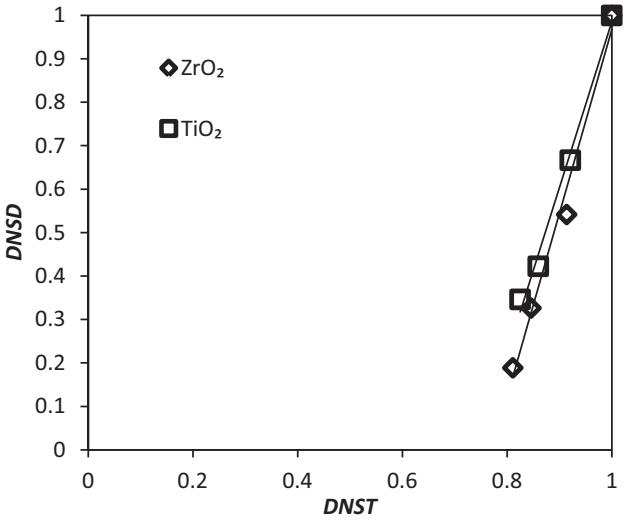

Fig. 6. *DNSD* vs. *DNST* in ZrO_2 and TiO_2 nanofluids.

cles (<0.01 wt%) help to sharply reduce the *ONT*. Also, the figure demonstrates that the *ONT* of 0.04wt% ZrO_2 and TiO_2 get advanced by 61% and by 58%, respectively. The *ONT* of nanofluids apparently decreases with increasing the nanoparticle concentrations until it becomes approximately constant. This occurs because according to the heterogeneous nucleation theory, nanoparticles make preferential sites for solidification. Therefore firstly, an increase in nanoparticle concentration leads to a higher nucleation rate; then, loading more nanoparticles causes hindering of nuclei growth and *ONT* becomes slightly constant. The increase in nanoparticle concentration illustrates a nonlinear enhancement behavior at *ONT* and a near linear enhancement in the *ST*. From the results of Fig 7, it is revealed that *ST* variation of ZrO_2 and TiO_2 at various nanoparticle concentrations is negligible. Even though ZrO_2 nanofluid provides slightly faster solid layers formation in solidification process. The *ST* of ZrO_2 and TiO_2 nanofluids with concentration of 0.04%, can be saved by nearly 19%.

Volumetric free energy as an effective parameter in solidification versus nanoparticle concentrations of ZrO_2 and TiO_2 is shown in Fig. 8. It is noticed that loading these nanoparticles present an enhancement in volumetric free energy at different nanoparticle concentrations. In other word, absolute value of volumetric free energy is reduced by nanoparticle concentration; which in accord with Eq. (4), causes the reduction of *SD*. As can be seen, the deceleration of absolute value of volumetric free energy induced by the ZrO_2 nanoparticle is higher than that of TiO_2. It occurs because although TiO_2 possesses higher thermal conductivity than ZrO_2, but ZrO_2 exhibits lower kinematic viscosity, thereby ZrO_2 nanoparticle has lower heat resistance and higher natural convection; which leads to acceleration of phase transition of ZrO_2 nanofluid. It is observed that various types and especially concentrations of nanoparticle would make remarkable impact on the volumetric free energy.

The variation of the critical nucleation radius with respect to nanoparticle concentration is observed in Fig. 9. These results of ZrO_2 and TiO_2 nanofluids show that an increase in nanoparticle concentration increases the critical nucleation radius.

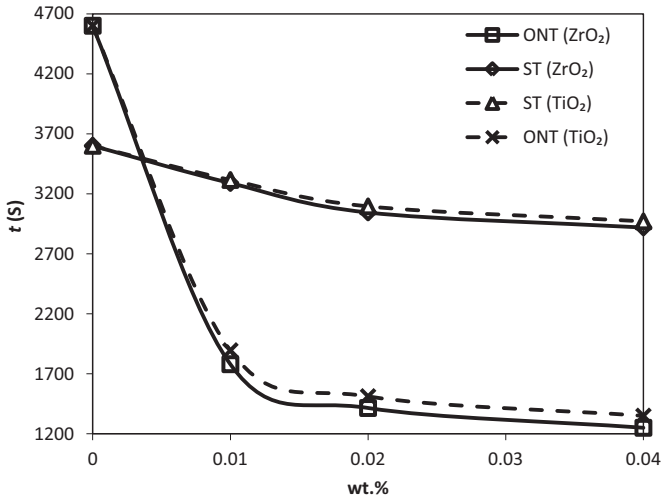

Fig. 7. Comparison of *ONT* and *ST* between ZrO_2 and TiO_2 nanofluids with respect to nanoparticle concentration.

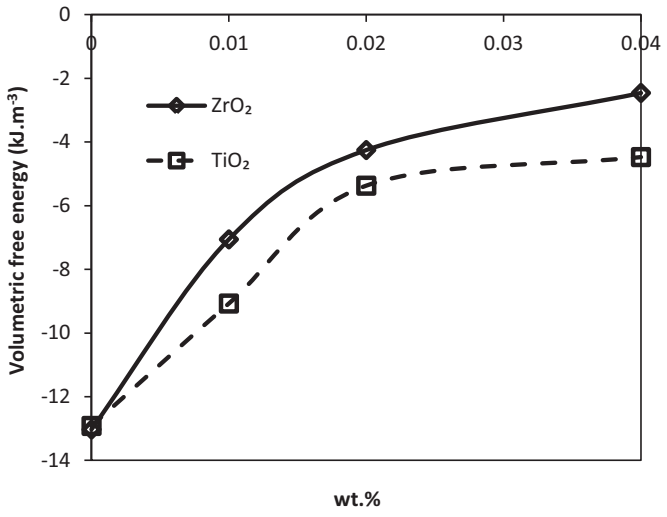

Fig. 8. Variation of volumetric free energy between ZrO_2 and TiO_2 nanofluids.

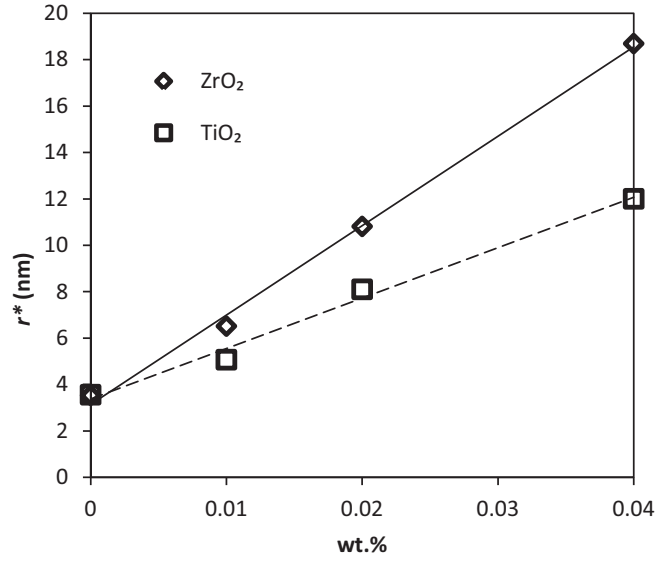

Fig. 9. The critical nucleation radius as a function of nanoparticle concentration for ZrO_2 and TiO_2 nanofluids.

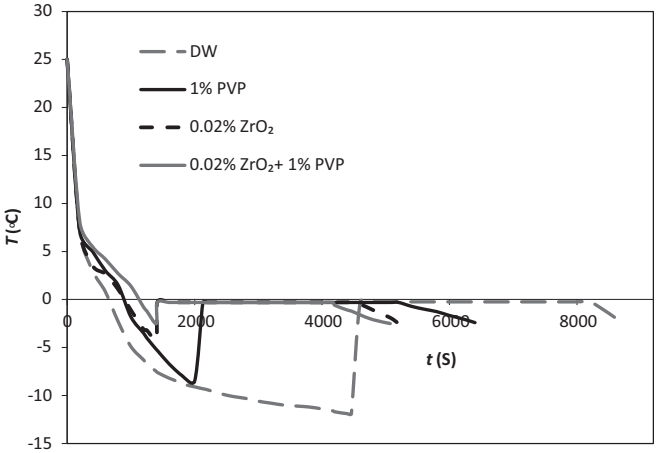

Fig. 10. Cooling curve of ZrO_2 nanofluids with and without surfactant.

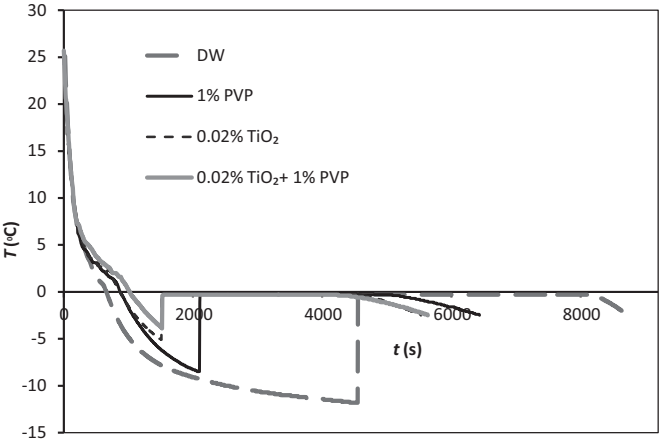

Fig. 11. Cooling curve of TiO_2 nanofluids with and without surfactant.

Also, enhancement of critical nucleation radius in the case of ZrO_2 nanofluid is consistently much more rapidly than that of TiO_2 nanofluids (nearly 2 times higher). It is evident that the r^* difference between ZrO_2 and TiO_2, becomes obvious along with enhanced concentration. As can be seen, when the nanoparticles concentrations of ZrO_2 and TiO_2 become 0.04 wt%, their critical nucleation radiuses begin to increase linearly up to almost 20 nm and 10 nm, respectively. These experimental results are fitted by the Eqs. (13) and (14) for ZrO_2 and TiO_2 in the range of wt% <0.04%:

$$r^*_{ZrO_2} = 385 * \text{wt\%} + 3.15,\ R^2 = 0.9969,\ \text{Accuracy} = \pm 7\% \quad (13)$$

$$r^*_{TiO_2} = 217 * \text{wt\%} + 3.38,\ R^2 = 0.9901,\ \text{Accuracy} = \pm 9\% \quad (14)$$

4.3. Solidification process of ZrO_2 and TiO_2 nanofluids with PVP as surfactant

In this section, the experimental study was conducted in order to assess the effects of surfactant, nanoparticle and their composition on solidification behavior of DW as basefluid. In turn, temperature variations of ZrO_2 and TiO_2 with and without surfactant are depicted in Figs. 10 and 11, respectively. It is clearly found that nanoparticle, surfactant and their composition can improve solidification behavior. As can be seen, time wise variations of ZrO_2 and TiO_2 nanofluid with and without surfactant follows the same trend. The *ONT* is found to be same for nanofluids with and without surfactant. It can be attributed to the simultaneous presence of both

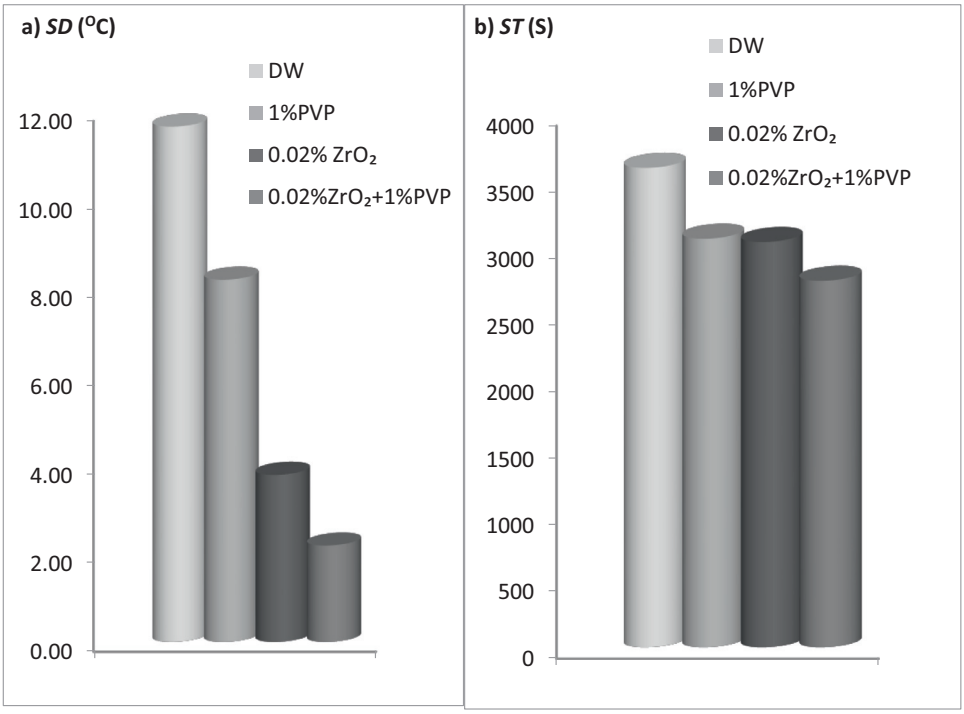

Fig. 12. Solidification characteristics of ZrO_2 nanofluids with and without surfactant.

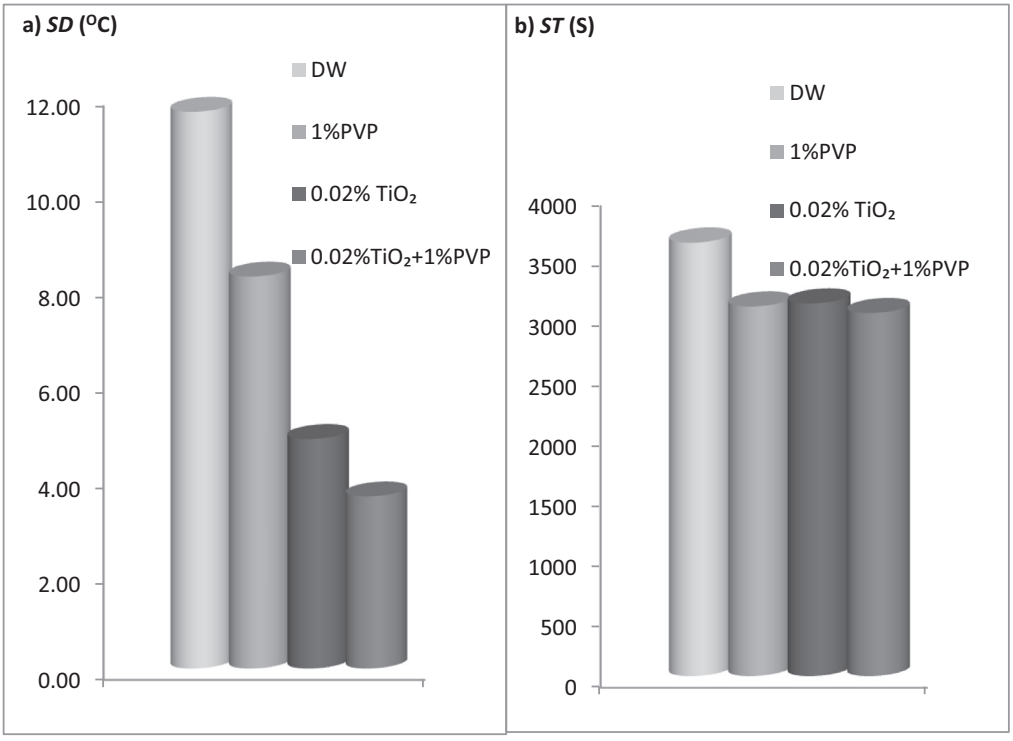

Fig. 13. Solidification characteristics of TiO_2 nanofluids with and without surfactant.

surfactant and nanoparticle which served as crystal growth retardant due to local confinement effect (Fan et al., 2015), despite of mixed response in the field of nucleating agent of nanoparticle and surfactant. The *ONT* of ZrO_2 and TiO_2 nanofluid (with/without PVP) are ahead of 1410 and 1530 s, respectively. Adding 1 wt% of PVP to basefluid can reduce *ONT* By 52%. It is due to the fact that the mechanisms of nucleating agent and contact angle are dominant in controlling solidification behavior of PVP and play their role on solidification. Adding PVP, by reduction of contact angle and enhancement of nucleating agent, provides higher nucleating sites for heterogeneous nucleation and leads to reduction in Gibbs free energy variation and consequently *SD* and *ONT*. On comparing the results of Figs. 10 and 11, the solidification characteristics of ZrO_2 and TiO_2 nanofluids are presented and discussed hereafter.

4.4. Comparison of solidification characteristics of ZrO_2 and TiO_2 nanofluids with PVP

Figs. 12 and 13, show the effect of nanoparticles, surfactant and their mixed response on *SD* and *ST*. The prevailing ef-

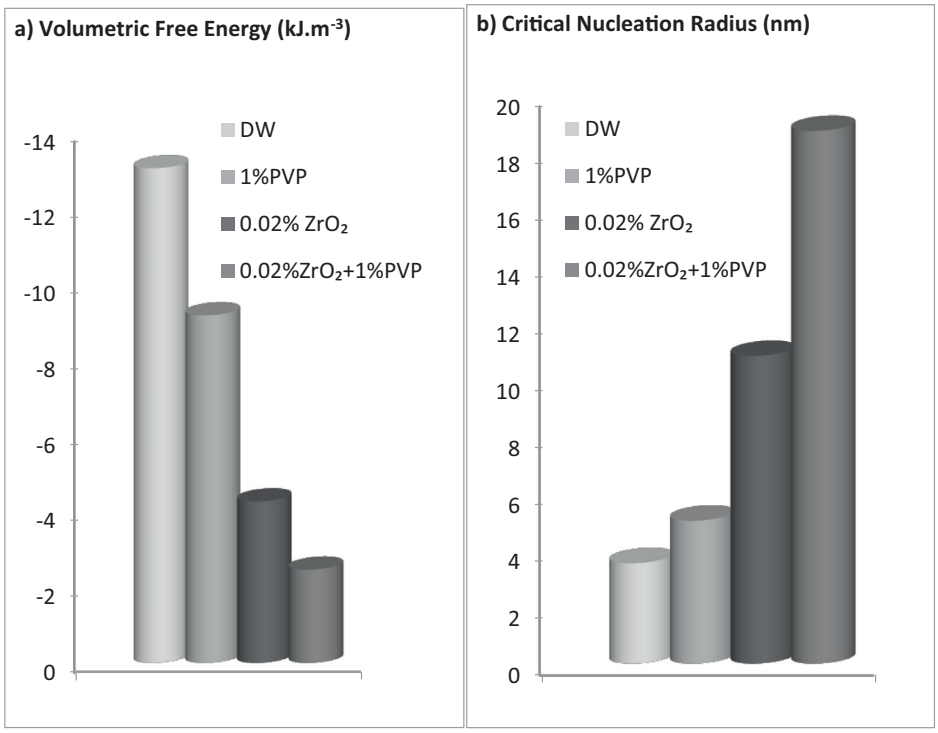

Fig. 14. (a) Volumetric free energy and (b) critical nucleation radius of ZrO_2 nanofluids with and without surfactant.

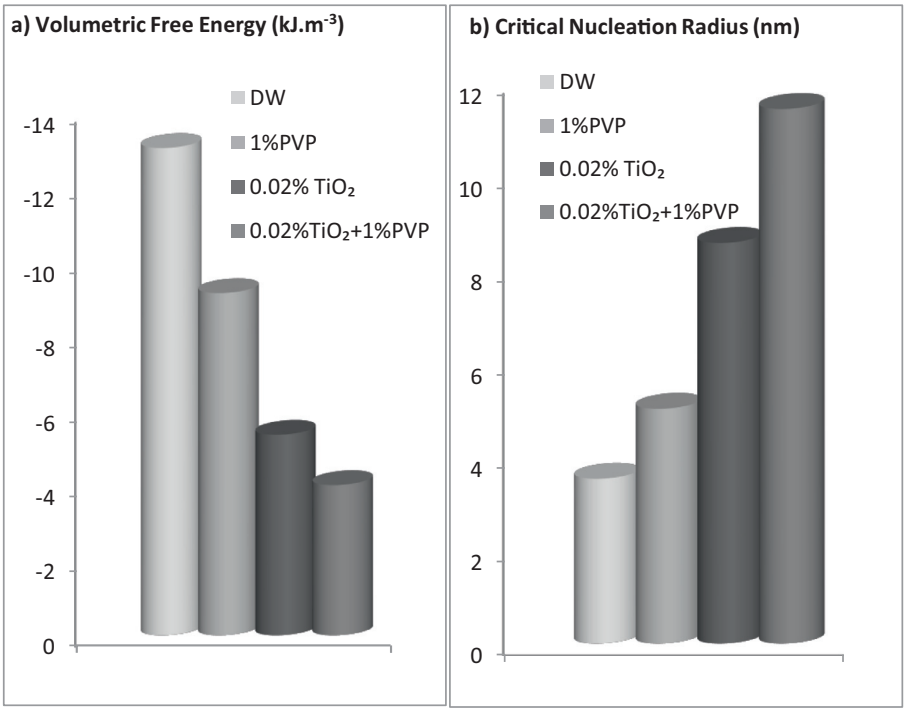

Fig. 15. (a) Volumetric free energy and (b) critical nucleation radius of TiO_2 nanofluids with and without surfactant.

fect of nanoparticle additives in basefluid compared to that of surfactant–even at higher concentration–upon *SD*, is clearly evident in Figs. 12 and 13. *SD* is greatly affected by metal oxide nanoparticles and slightly by surfactant. As expected, minimum *SD* and *ST* are detected when both surfactant and nanoparticle are dispersed in basefluid. It occurs because the *SD* and *ST* of nanofluids with/without surfactant are influenced by changing contact angle (Jia et al., 2014) and changing surface free energy which occupy a high proportion of total energy of system (due to the change in molecular arrangement of liquid in the film, along with the solidification process) (He et al., 2012). Also, it could be owing to the collision and mutual interference between the nanoparticle and surfactant (Jia et al., 2014). Furthermore from the perspective of the heterogeneous nucleation (which is attributed to the nucleation area) due to enhancement of exposed surface area, the *SD* and *ST* for the case of DW + 1 wt% PVP+ nanoparticle is reduced when compared with that of DW+ nanoparticle. The results are in accordance with the studies of Jia et al. (2014). The *SD* of DW +PVP

is reduced by 30% and appreciably nanofluids+PVP are reduced by 82% for ZrO_2 and 70% for TiO_2, due to their enhanced heat transfer properties. It is construed that ZrO_2 and TiO_2 nanofluids+ surfactant allows the *ST* to degrade by 23% and 16%, respectively; which causes promotion of energy saving potential.

Figs. 14 and 15 illustrate the comparison of volumetric free energy and critical nucleation radius of base fluid and nanofluids with/without surfactant. The observation associated with Figs. 14 and 15 indicates that these solidification characteristics of composite PCM generally rely on the presence of nanoparticle, surfactant or their composition. It is noticed from the figures that as nanoparticle and/or surfactant are added to DW, the absolute value of volumetric free energy decreases. Generally, the results confirm that the higher r^* and lower volumetric free energy are contributed by nanofluids containing surfactant compared to that of DW. Obviously based on the results, it is interpreted that the co-presence of both nanoparticle and surfactant could promote heterogeneous nucleation by reducing the absolute value of volumetric free energy and enhancing critical nucleation radius of basefluid. A reduction percentage of volumetric free energy is about 81% and 69% for ZrO_2 and TiO_2, respectively. Lower volumetric free energy of DW+ surfactant by using ZrO_2 nanoparticle predicts an energy saving potential in energy storage system. The increase in r^*, in the case of ZrO_2 and TiO_2 with surfactant are 5 and 3 times higher than that of DW, respectively.

5. Concluding remarks

In order to evaluate and compare the effects of nanoparticle concentration on nanofluid solidification process, the experimental investigation using ZrO_2 and TiO_2 nanofluids with/ without surfactant were conducted. Based on the presented results, the major findings in this paper were as follows:

- ZrO_2 nanofluid contributes to faster reduction in supercooling degree and time of solidification (as important parameters in solidification process) compared with TiO_2 nanofluid.
- The dominant mechanism beyond lower supercooling degree of ZrO_2 compared to TiO_2, is due to the lower kinematic viscosity of ZrO_2.
- Enhancement in critical nucleation radius of ZrO_2 nanofluid occurs much more quickly than that of TiO_2 nanofluid.
- The presence of PVP as surfactant in ZrO_2 and TiO_2 nanofluids would results a corresponding decrease in supercooling degree, solidification time and absolute volumetric free energy and increase in critical nucleation radius.
- The effect of PVP as stabilizer on *ONT* of ZrO_2 and TiO_2 nanofluids is not actually significant.
- The comparison of ZrO_2 solidification results with those of TiO_2 implies that ZrO_2 has more energy saving potential to be applied to storage systems.

Acknowledgment

The authors gratefully acknowledge the financial support from the Ferdowsi University of Mashhad and Iranian Nanotechnology Initiative Council.

References

Abdollahzadeh, M., Esmaeilpour, M., 2015. Enhancement of phase change material (PCM) based latent heat storage system with nanofluid and wavy surface. Int. J. Heat Mass Transf. 80, 376–385.
Altohamy, A.A., Abd Rabbo, M.F., Sakr, R.Y., Attia, A.A., 2015. Effect of water based Al_2O_3 nanoparticle PCM on cool storage performance. Appl. Therm. Energy 84, 331–338.
Aslani, H., Moghiman, M., 2015. Experimental investigation and fuzzy logic modelling of nanofluid solidification behavior. Modares Mech. Eng. 15, 284–292 (In Persian).
Azmi, W.H., Sharma, K.V., Mamat, R., Najafi, G., Mohamad, M.S., 2016. The enhancement of effective thermal conductivity and effective dynamic viscosity of nanofluids – a review. Renew. Sustain. Energy Rev. 53, 1046–1058.
Bavand, M., Rashidi, S., Esfahani, J.A., 2015. Enhancement of heat transfer by nanofluids and orientations of the equilateral triangular obstacle. Energy Convers. Manag. 97, 212–223.
Chandrasekaran, P., Cheralathan, M., Kumaresan, V., Velraj, R., 2014a. Solidification behavior of water based nanofluid phase change material with a nucleating agent for cool thermal storage system. Int. J. Refrig. 41, 157–163.
Chandrasekaran, P., Cheralathan, M., Kumaresan, V., Velraj, R., 2014. Enhanced heat transfer characteristics of water based copper oxide nanofluid PCM (phase change material) in a spherical capsule during solidification for energy efficient cool thermal storage system. Energy 72, 636–642.
Du, Y., Ding, Y., 2017. Optimization of cold storage efficiency in a rankine-cycle-based cold energy storage system. Energy Technol. 5, 267–276.
Elmozughi, A.F., Solomon, L., Oztekin, A., Neti, S., 2014. Encapsulated phase change material for high temperature thermal energy storage – heat transfer analysis. Int. J. Heat Mass Transf. 78, 1135–1144.
Fan, L.W., Yao, X.L., Wang, X., Wu, Y.Y., Liu, X.L., Xu, X., Yu, Z.T., 2015. Non-isothermal crystallization of aqueous nanofluids with high aspect-ratio carbon nano-additives for cold thermal energy storage. Appl. Energy 138, 193–201.
Golestaneh, S.I., Mosallanejad, A., Karimi, G., Khorram, M., Khashi, M., 2016. Fabrication and characterization of phase change material composite fibers with wide phase-transition temperature range by co-electrospinning method. Appl. Energy 182, 409–417.
Gunther, E., Huang, L., Mehling, H., Dotsch, C., 2011. Subcooling in PCM emulsions-Part 2: Interpretation in terms of nucleation theory. Thermochim. Acta 522 (1), 199–204.
Harikrishnan, S., Magesh, S., Kalaiselvam, S., 2013. Preparation and thermal energy storage behaviour of stearic acid–TiO_2 nanofluids as a phase change material for solar heating systems. Thermochim. Acta 565, 137–145.
He, Q., Wang, S., Tong, M., Liu, Y., 2012. Experimental study on thermophysical properties of nanofluids as phase-change material (PCM) in low temperature cool storage. Energy Convers. Manag. 64, 199–205.
Ismail, K.A.R., Filho, L.M.S., Lino, F.A.M., 2012. Solidification of PCM around a curved tube. Int. J. Heat Mass Transf. 55, 1823–1835.
Jia, L., Peng, L., Chen, Y., Mo, S., Li, X., 2014. Improving the supercooling degree of titanium dioxide nanofluids with sodium dodecylsulfate. Appl. Energy 124, 248–255.
Khodadadi, J.M., Fan, L., Babaei, H., 2013. Thermal conductivity enhancement of nanostructure-based colloidal suspensions utilized as phase change materials for thermal energy storage: a review. Renew. Sustain. Energy Rev. 24, 418–444.
Kim, T.I., Chang, W.J., Chang, S.H., 2011. Flow boiling CHF enhancement using Al_2O_3 nanofluid and an Al_2O_3 nanoparticle deposited tube. Int. J. Heat Mass Transf. 54, 2021–2025.
Kumaresan, V., Velraj, R., Das, S.K., 2012. Convective heat transfer characteristics of secondary refrigerant based CNT nanofluids in a tubular heat exchanger. Int. J. Refrig. 35, 2287–2296.
Kumaresan, V., Chandrasekaran, P., Nanda, M., Maini, A.K., Velraj, R., 2013. Role of PCM based nanofluids for energyefficient cool thermal storage system. Int. J. Refrig. 36 (6), 1641–1647.
Lei, J., Yang, J., Yang, E.H., 2016. Energy performance of building envelopes integrated with phase change materials for cooling load reduction in tropical Singapore. Appl. Energy 162, 207–217.
Li, G., Hwang, Y., Radermacher, R., Chun, H.H., 2013. Review of cold storage materials for subzero applications. Energy 51, 1–17.
Liu, Y., Li, X., Hu, P., Hu, G.A., 2015. Study on the supercooling degree and nucleation behavior of water-based graphene oxide nanofluids PCM. Int. J. Refrig. 50, 80–86.
Lu, W., Tassou, S.A., 2012. Experimental study of the thermal characteristics of phase change slurries for active cooling. Appl. Energy 91 (1), 366–374.
Mahbubul, I.M., Saidur, R., Amalina, M.A., 2013. Influence of particle concentration and temperature on thermal conductivity and viscosity of Al_2O_3/R141b nanorefrigerant. Int. Commun. Heat Mass Transf. 43, 100–104.
Mo, S., Chen, Y., Jia, L., Luo, X., 2012. Investigation on crystallization of TiO_2–water nanofluids and deionized water. Appl. Energy 93, 65–70.
Mo, S., Chen, Y., Cheng, Z., Jia, L., Luo, X., Shao, X., Yuan, X., Lin, G., 2015. Effects of nanoparticles and sample containers on crystallization supercooling degree of nanofluids. Thermochim. Acta 605, 1–7.
Moghiman, M., Aslani, B.H., 2013. Influence of nanoparticles on reducing and enhancing evaporation mass transfer and its efficiency. Int. J. Heat Mass Transf. 61, 114–118.
Nomura, T., Zhu, C., Nan, S.h., Tabuchi, K., Wang, Sh., Akiyama, T., 2016. High thermal conductivity phase change composite with a metal-stabilized carbon–fiber network. Appl. Energy 179, 1–6.
Raja, M., Vijayan, R., Dineshkumar, P., Venkatesan, M., 2016. Review on nanofluids characterization, heat transfer characteristics and applications. Renew. Sustain. Energy Rev. 64, 163–173.
Sarafraz, M.M., Kiani, T., Hormozi, F., 2016. Critical heat flux and pool boiling heat transfer analysis of synthesized zirconia aqueous nano-fluids. Int. Commun. Heat Mass Transf. 70, 75–83.
Sari, A., Alkan, C., Bilgin, C., 2014. Micro/nano encapsulation of some paraffin eutectic mixtures with poly(methyl methacrylate) shell: preparation, characterization and latent heat thermal energy storage properties. Appl. Energy 136, 217–227.
Teng, T.P., 2013. Thermal conductivity and phase change properties of aqueous alumina nanofluid. Energy Convers. Manag. 67, 369–375.

Wang, X.J., Li, X.F., Xu, Y.H., Zhu, D.S., 2014. Thermal energy storage characteristics of Cu–H_2O nanofluids. Energy 78, 212–217.
Wang, H., Wang, F., Li, Z., Tang, Y., Yu, B., Yuan, W., 2016a. Experimental investigation on the thermal performance of a heat sink filled with porous metal fiber sintered felt_paraffin composite phase change material. Appl. Energy 176, 221–232.
Wang, T., Wang, Sh., Geng, L., Fang, Y., 2016b. Enhancement on thermal properties of paraffin/calcium carbonate phase change microcapsules with carbon network. Appl. Energy 179, 601–608.
Williams, W.C., Buongiorno, J., Hu, L.W., 2008. Experimental investigation of turbulent convective heat transfer and pressure loss of alumina/water and zirconia/water nanoparticle colloids (nanofluids) in horizontal tubes. J. Heat Transf. 130, 424121–424127.
Wu, S., Zhu, D., Li, X., Li, H., Lei, J., 2009. Thermal energy storage behavior of Al_2O_3–H_2O nanofluids. Thermochim. Acta 483 (1), 73–77.
Yamanaka, S., Ito, N., Akiyama, K., Shimosaka, A., Shirakawa, Y., 2012. Heterogeneous nucleation and growth mechanism on hyrophilic and hydrophobic surface. Adv. Power Tech. 23 (2), 268–272.
Yiamsawasd, Th., Dalkilic, A.S., Wongwises, S., 2012. Measurement of the thermal conductivity of titania and alumina nanofluids. Thermochim. Acta 545, 48–56.
Zabalegui, A., Lokapur, D., Lee, H., 2014. Nanofluid PCMs for thermal energy storage: latent heat reduction mechanisms and a numerical study of effective thermal storage performance. Int. J. Heat Mass Transf. 78, 1145–1154.
Zeng, Y., Fan, L.W., Xiao, Y.Q., Yu, Z.T., Cen, K.F., 2013. An experimental investigation of melting of nanoparticle-enhanced phase change materials (NEPCMs) in a bottom-heated vertical cylindrical cavity. Int. J. Heat Mass Transf. 66, 111–117.
Zhang, X.J., Wu, P., Qiu, L.M., Zhang, X.B., Tian, X.J., 2010. Analysis of the nucleation of nanofluids in the ice formation process. Energy Convers. Manag. 51, 130–134.
Zhao, W., Elmozughi, A.F., Oztekin, A., Neti, S., 2013. Heat transfer analysis of encapsulated phase change material for thermal energy storage. Int. J. Heat Mass Transf. 63, 323–335.